

Modelling the Effect of Room Temperature Storage and Deformation on the Age-hardening Behaviour of Al-Mg-Si alloys

C. Schäfer¹, O.R. Myhr², Z. Liang³, H.J. Brinkman¹, O. Engler¹, J. Hirsch¹, C. Chang⁴,
J. Banhart^{3,4}

¹ Hydro Aluminium Rolled Products GmbH, Research and Development Bonn,
53014 Bonn, Germany.

² Hydro Aluminium, Research and Technology Development, N-6601 Sunndalsøra, Norway.

³ Helmholtz Zentrum Berlin für Materialien und Energie, 14109 Berlin, Germany.

⁴ Technische Universität, 10623 Berlin, Germany.

Keywords: Modelling, Precipitation, Al-Mg-Si, automotive sheet

Abstract

The present investigation deals with modelling of the age-hardening behaviour of 6XXX series automotive sheet alloys. The basis for the work is a precipitation model developed for coupled nucleation, growth, dissolution and coarsening in Al-Mg-Si extrusion alloys. It has been advanced to incorporate the important effects of room temperature (RT) storage and deformation prior to the final age-hardening. The model predicts the evolution of the precipitate structure and the corresponding RT yield strength for non-isothermal heat treatments. The model validation is based on both a comprehensive set of tensile tests and TEM measurements on selected samples. A comparison between model predictions and measurements shows reasonable agreement, and it is concluded that after some further development, the model can be used as an industrial tool for process chain simulations of the yield strength response following complex heat treatments and deformation schedules.

1. Introduction

The artificial ageing of Al-Mg-Si sheet alloys is of significant practical relevance in the automotive industry where these alloys are used for body-in-white applications. These alloys are subjected during their processing not only to different heat treatments, but also to RT storage and deformation, which strongly influence the age-hardening response of the material and hence the mechanical properties. During artificial ageing Al-Mg-Si alloys undergo complex structural changes caused by precipitation, static recovery in pre-strained samples and reactions between solute atoms and vacancies. Their extent strongly depends on the temperature and the time the material is exposed to this temperature. A natural ageing (due to RT storage) and a subsequent deformation (due to part forming) will further modify the precipitation sequence due to the formation of early phases and the heterogeneous nucleation at dislocations.

Such complex material behaviour is very hard to predict, but its modelling highly desirable, in order to tailor material properties, for which the treatments are partially associated with the customer process. For this purpose, the precipitation model NaMo [1-4] was advanced and applied to simulate the above mentioned effects.

2. Experimental

The present investigation was conducted on a 1.15 mm thick AA 6960 sheet which is a typical alloy used for automotive applications. The sheet was produced on commercial production lines

at the AluNorf rolling mill in Norf, Germany, and finally was subjected to a laboratory solution treatment, as well as ageing treatments at the Hydro Research and Development Centre in Bonn. The solution heat treatment was carried out in a fluidized sand bath at 560°C for 5 min, with a heating rate of 12°C/s and a temperature variation of $\pm 2^\circ\text{C}$. After the solution heat treatment the material was water quenched to RT to keep a high amount of Mg and Si in solid solution. Two different routes of ageing treatments were applied (see inlay in Fig. 1 (b)). For route A, the solutionized material was stored at RT for various times t_1 ranging from 35 sec up to 2 months prior to the artificial ageing treatment at 185°C and 205°C in an oil bath with minor temperature variation of $\pm 0.2^\circ\text{C}$. Both ageing temperatures are commonly used to mimic the paint bake cycle. In another route (B), selected samples were taken after different RT storage times t_1 , strained to 10% and stored another hour ($=t_2$) at RT before being subjected to artificial ageing.

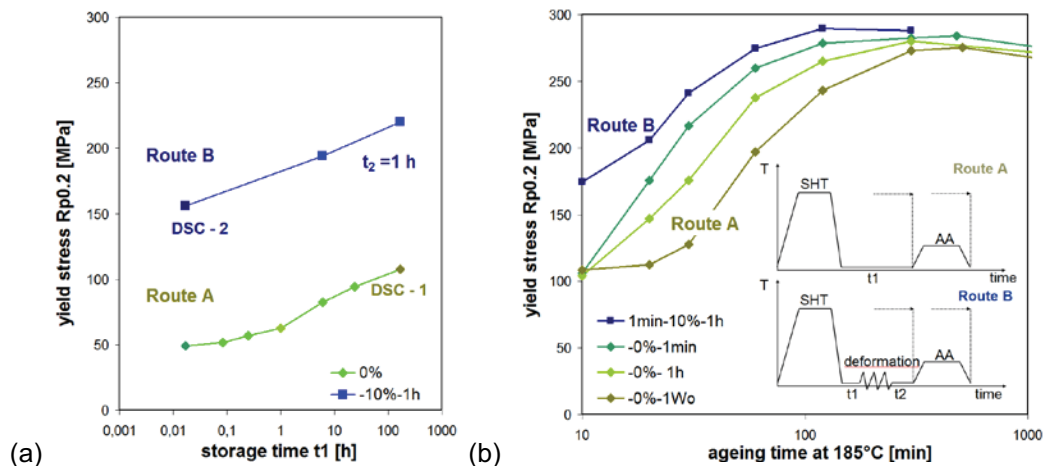


Figure 1. Experimental yield stress data for the considered alloy after solution heat treatment and (a) RT storage (route A), respectively RT storage and deformation (route B); (b) and artificial ageing at 185°C. AA= artificial ageing; SHT= solution heat treatment; RT=room temperature.

Fig. 1 (a) displays the yield stress evolution during natural ageing with and without deformation (route B and A). For route A material the yield stress is increasing during natural ageing, with a significant rise between 15 min and 6 h. Material from route B shows a similar increase in the yield strength, but on a much higher level due to additional strain hardening.

A subsequent artificial ageing treatment at 185°C (Fig. 1 (b)) leads for route A material to an additional increase of yield strength to values up to 270 MPa due to precipitation hardening. With increasing RT storage time, the precipitation kinetics is shifted to longer ageing times. In comparison, route B material experiences during artificial ageing a pronounced acceleration of the precipitation kinetics and reaches higher peak strength (Fig. 1 (b), blue curve). However, the relative contribution of precipitation hardening in the pre-deformed samples decreased.

Differential scanning analysis was employed for the identification of the precipitates developed during artificial ageing for selected samples (indicated in Fig. 1 (a) by numbers). For sample 1 ($t_1=1$ week RT storage) an exothermal reaction is obtained at 240°C, which can be attributed to the formation of β'' [14], which is confirmed by the TEM micrographs in Fig. 2 (a, b). For material 10% pre-strained during natural ageing (route B) prior to artificial ageing (sample 2), the formation of β'' , β' can be observed in agreement with literature [13, 14]. The β' precipitates are the rod-shaped precipitates [13, 14] indicated in Fig. 2 (c). Additionally, Cu-containing particles, presumably Q' particles were observed [12].

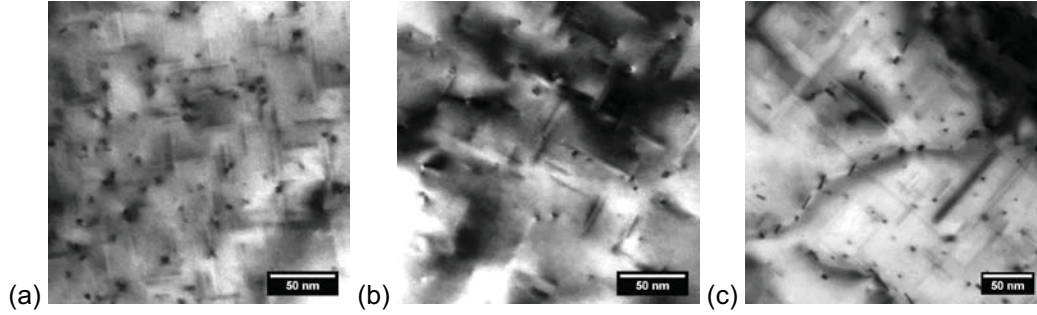


Figure 2. TEM micrographs of the alloy after RT storage for 3.5 weeks and artificial ageing at 205°C; (a) After 30 min artificial ageing - fine phases β'' , (b) after 90 min ageing - coarse phases β'' , (c) after pre-straining for 10% and artificially ageing for 90 min at 205°C - β'' , β' and Q' precipitates.

3. Modelling

The microstructure model by Myhr and Grong named NaMo [1-4], originally developed for extrusion alloys, was employed to model the age hardening behaviour of the relevant Al-Mg-Si sheet alloy. NaMo comprises several submodels, i.e. a precipitation, a yield stress and a work-hardening model [4]. Details of the underlying assumptions as well as a description of the mathematical framework and solution algorithms are given in [1-4]. The objective of the present work is to further develop and apply the model for predictions of the effect of RT storage and plastic deformation on the age hardening response. This requires several new features to be included in the model, i.e. the introduction of a separate particle size distribution for GP-zones, an additional nucleation law for precipitation on dislocations, and a static recovery model for predictions of the annihilation of dislocations during the heat treatment as outlined below.

Nucleation

In the present modelling, precipitates are assumed to form either finely distributed within the matrix (GP-zones and β'' -particles) or heterogeneously along the dislocation line (β' -particles). For the former type of precipitates, the following nucleation law which includes the effect of quenched-in vacancies established at the local peak temperature, is applied [2, 3].

$$j = j_0 \frac{C_v}{C_v^{ref}} \exp\left(-\frac{\Delta Q_d}{RT}\right) \exp\left(-\frac{\Delta G^*}{RT}\right) \quad (1)$$

Here the parameter j_0 is a constant, C_v and C_v^{ref} are the vacancy concentration in the matrix for the actual alloy and for a reference material, respectively, Q_d is the activation energy for diffusion, R and T are the ideal gas constant and the absolute temperature, respectively, and ΔG^* is the energy barrier for nucleation. By including the effect of elastic coherency strains around the nucleated particles, an appropriate expression for the energy barrier for heterogeneous nucleation is [1-3].

$$\Delta G^* = \frac{(A_0)^3}{(RT \ln(\bar{C}/C_e) - \Delta G_s)^2} \quad (2)$$

Here, \bar{C} is the mean solute content in the matrix and C_e is the equilibrium solute concentration as given by the phase diagram. The misfit strain energy ΔG_s can be estimated as described in [5], and in the present work a reasonable value of 21.0 kJ/mol was applied.

For samples subjected to cold deformation prior to the ageing heat treatment, particles may heterogeneously nucleate on dislocations. Following Deschamps [6], a rough estimate of the number density N_l of such nucleation sites can be obtained as follows:

$$N_l = \frac{\rho}{L_l} \quad (3)$$

where ρ is the dislocation density, and L_l is the average distance between nucleation sites along the dislocation line. In the present work, L_l was estimated from TEM micrographs showing precipitation of β' -particles along dislocations. From Fig. 2(c), a typical value of 35 nm was found, and used as a basis for the simulations.

Rate law

After a nucleus has been introduced into the system, it will either grow or dissolve, depending on whether the particle / matrix interface concentration C_i exceeds the mean matrix concentration \bar{C} or not. The rate at which this occurs can be expressed as [7]

$$\frac{dr}{dt} = \frac{\bar{C} - C_i}{C_p - C_i} \frac{D}{r} \quad (4)$$

where r is the particle radius, C_p the solute concentration within the particle and D the diffusion coefficient. In the presence of dislocations, precipitation kinetics is accelerated due to pipe diffusion through the dislocation core which is significantly faster than matrix bulk diffusion, and can be expressed by an efficient diffusion coefficient D_{eff} which replaces D in Eq. (4) [5, 8].

$$D_{eff} = D_v \left(1 + \rho a_c \frac{D_{c0}}{D_{v0}} \right) \exp\left(\frac{\Delta Q}{RT} \right) \quad (5)$$

Here D_v is the volume diffusion coefficient, a_c the cross-sectional area of the pipes, D_{v0} and D_{c0} are the pre-exponential constants in the diffusion equation for bulk and core diffusion, respectively, while $\Delta Q = Q_d - Q_c$ is the difference in activation energy between bulk and core diffusion. The following values from Poole et al [8] were used in the simulations:

$$\Delta Q = 40 \text{ kJ/mol and } a_c \frac{D_{c0}}{D_{v0}} = 4.7 \cdot 10^{-19} \text{ m}^2.$$

Yield strength and static recovery

In the present modelling we assume that the individual strength contributions, i.e. intrinsic yield strength, solid solution, precipitation hardening and hardening from dislocations, can be added linearly. The initial dislocation density ρ as well as the corresponding hardening contribution are estimated from the applied plastic strain. During the ageing, ρ will continuously decrease due to static recovery, and a reasonable expression for the reaction rate is [9, 10]:

$$\frac{d\rho}{dt} = -v_D B_\rho l_g \rho^{3/2} \exp\left(-\frac{U_s}{kT}\right) 2 \sinh\left(\frac{Gb^3 l_j \sqrt{\rho}}{kT}\right) \quad (6)$$

Here v_D is the Debye frequency, B_ρ is a constant, l_g is the mean free length the dislocation moves per thermal jump, l_j is the activated length, which depends on the solute concentration, k is the Boltzmann constant and U_s is the activation energy for solute diffusion. In practice, the material dependent constants in Eq. (6) must be known beforehand. In the present work, the parameters were tuned to obtain a good fit to measured dislocation densities reported in [11] for a typical Al-Mg-Si alloy.

Comparison between predictions and experiments

From the experiments described in Fig. 1, two different processing routes (i.e. Route A and B) were simulated using the above outlined model. Fig. 3 (a) shows a comparison between the predicted and measured yield stress evolution during RT storage (route A). The predicted natural ageing behaviour corresponds closely to the experimental results. The model simulations for the sample subjected to natural ageing for one week prior to the age-hardening (Fig. 3 (b)) indicate an initial drop in yield stress due to the dissolution of Mg/Si-clusters and GP-zones. The subsequent increase in strength is caused by precipitation of β'' -particles (Fig. 3 (b)) and is slightly faster than observed in the experiments, but reaches nevertheless excellent agreement in the peak-strength.

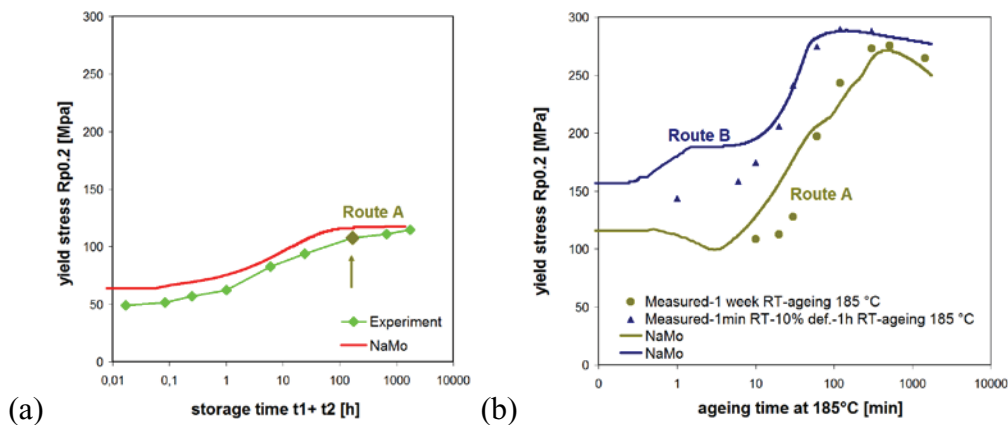


Figure 3. Simulated yield stress evolution during (a) RT storage (route A) and (b) artificial ageing (route A and B), modelled with the precipitation model NaMo.

Fig. 3(b) shows the yield strength evolution during artificial ageing for the material subjected to 10% plastic strain 1 minute after quenching from the solid solution temperature (route B). The overall agreement between calculated and measured yield strength is reasonable, except for the predicted sudden increase of the strength between 1 and 10 min caused by the assumption of site saturation giving a too fast growth rate during the first part of the ageing heat treatment. Fig. 4 shows the predicted evolution of the individual hardening contributions for samples that were 10% deformed 1 minute after quenching from the solid solution temperature (i.e. Route B).

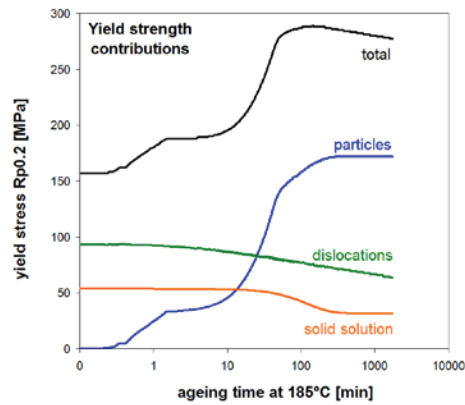


Figure 4. Predicted evolution of the individual hardening contributions from elements in solid solution, dislocations and particles during artificial ageing for samples that were 10% deformed 1 minute after quenching from the solid solution temperature.

4. Summary and Conclusions

A precipitation model for 6XXX sheet alloys was presented and applied to model the yield strength evolution during various natural and artificial ageing heat treatments, including pre-deformation at room temperature. This required firstly, the consideration of heterogeneous nucleation of β' particles at dislocations and increased diffusion rates due to pipe diffusion along the dislocation cores, and secondly, the introduction of recovery to describe the annihilation of dislocations during annealing. The comparison to experimental data shows that the model captures the main effects of pre-deformation and room temperature storage reasonably well, even though some further development is required to capture the effect of solute-vacancy interactions on the age-hardening.

References

1. O. R. Myhr and Ø. Grong, *Acta Materialia*, 48 (2000), 1605.
2. O. R. Myhr, Ø. Grong, S. J. Anderson, *Acta Materialia*, 49 (2001), 65.
3. O. R. Myhr, Ø. Grong, H.G. Fjær, C. D. Marioara, *Acta Materialia*, 52 (2004), 4997.
4. O. R. Myhr, Ø. Grong, and K. O. Pedersen: *Metallurgical Trans. A*, 41 (9) (2010), 2276.
5. D. A. Porter and K. E. Easterling, *Phase Transformations in Metals and Alloys*, (Wokingham (England): Van Nostrand Reinhold Co. Ltd., 1981), 102.
6. A. Deschamps, Y. Bréchet, *Acta Materialia*, 47 (1999), 293.
7. H. B. Aaron, D. Fainstain, and G. R. Kotler, *J. Appl. Physics*, 41 (1970), 4404.
8. W. J. Poole, H. R. Shercliff, T. Castillo, *Material Science and Technology*, 13 (1997), 897.
9. E. Nes, *Acta Metallurgica Materialia*, 43 (1995), 2189.
10. J. A. Sæter, B. Forbord, H. E. Vatne and E. Nes: in Proc. of the 6th International Conference on Aluminium Alloys, 1 (1998), 113.
11. T. Furu, Ø. Ryen and O. R. Myhr: in Proc. of the 11th International Conference on Aluminium Alloys, 1 (2008), Aachen, Germany, 1626.
12. A. Gaber, A. Mossad Ali, K. Matsuda, T. Kawabata, T. Yamazaki, S. Iken, *J. of Alloys and Compounds*, 432 (2007), 149.
13. M. H. Jacobs, *Philosophical Magazine*, 26 (1972), 1.
14. N. Maruyama, R. Uemori, N. Hashimoto, M. Saga, M. Kikuchi, *Scripta Materialia*, 36 (1997), 89.